



## Short Communication

## X-ray diffraction and the symmetry of ultrathin crystalline materials between two-dimensional and three-dimensional crystals

Hengrui Ma<sup>a,1</sup>, Qiaorong Jiang<sup>a,1</sup>, Zi-Ang Nan<sup>a,\*</sup>, Gen Li<sup>a</sup>, Yanyan Jia<sup>b</sup>, Ruoxin Ning<sup>a</sup>, Jia-Bao Ji<sup>c</sup>, Zhenming Cao<sup>a</sup>, Linzhe Lü<sup>a</sup>, Huiqi Li<sup>a</sup>, Sheng Dai<sup>b</sup>, Haixin Lin<sup>a,d,\*</sup>, Zhaoxiong Xie<sup>a,d,\*</sup>

<sup>a</sup> State Key Laboratory of Physical Chemistry of Solid Surfaces, Collaborative Innovation Center of Chemistry for Energy Materials, and Department of Chemistry, College of Chemistry and Chemical Engineering, Xiamen University, Xiamen 361005, China

<sup>b</sup> Key Laboratory for Advanced Materials and Feringa Nobel Prize Scientist Joint Research Center, Institute of Fine Chemicals, School of Chemistry & Molecular Engineering, East China University of Science and Technology, Shanghai 200237, China

<sup>c</sup> Department of Chemistry and Applied Biosciences, Laboratory of Physical Chemistry, ETH Zürich, Zürich CH-8093, Switzerland

<sup>d</sup> Innovation Laboratory for Sciences and Technologies of Energy Materials of Fujian Province (IKKEM), Xiamen 361005, China

## ARTICLE INFO

## Article history:

Received 22 December 2022

Received in revised form 4 March 2023

Accepted 30 March 2023

Available online 6 April 2023

© 2023 Science China Press. Published by Elsevier B.V. and Science China Press. All rights reserved.

Following the precedent of graphene [1], ultrathin crystalline materials have displayed a broad range of fascinating properties, such as superconductivity, nonlinear optics, and piezoelectricity [2–7]. Generally, previous studies have ascribed them as ideal two-dimensional (2D) crystals or three-dimensional (3D) crystals thinned in one dimension, which cannot accurately describe the symmetries of the stacking forms for ultrathin crystalline materials. For ideal 2D crystals, they can be described by the 17 wallpaper groups with infinitely periodic 2D lattices, while bulk crystals are depicted by the 3D space groups. However, compared with 3D or ideal 2D crystals, ultrathin crystalline materials exhibit tunable degrees of freedom in the third direction, which are promising to exhibit unique properties owing to their symmetry variations. For example, the magic-angle twisted bilayer graphene can exhibit unconventional superconductivity by means of the layer twisting [2], and Pd nanosheets (NSs) can exhibit tunable intrinsic strain to optimize catalytic activity through the atomic layer control of thickness [5]. Therefore, it is not suitable to ascribe ultrathin crystalline materials to either ideal 2D or 3D crystals. On the other hand, it's well-known X-ray diffraction (XRD) of crystals is an essential characterization for the symmetry of crystalline materials. Owing to the unique freedom in the third dimension, the symmetries of ultrathin crystalline are different from that of ideal 2D or 3D crystals. However, the diffraction pattern differences between ultrathin crystalline materials and their bulk counterparts has gen-

erally been neglected in previous studies. Thus it's still challenging to make a comprehensive understanding of ultrathin crystalline materials, which requires us to re-examine this class of materials from a new perspective.

In this work, we prove that the powder XRD patterns differences between ultrathin crystalline materials and their 3D counterparts are related to the finite/non-periodic layers along the stacking direction. Three representative types of structures with different stacking characters are specifically discussed, including ultrathin characteristics (3-layer Rh NSs and 8-layer Pd NSs), periodicity destruction due to stacking faults (14-layer Ru NSs), and rotation between layers (twisted bilayer graphene) (Fig. 1). In order to elucidate the unique diffraction characteristics of ultrathin crystalline materials, a new full-structure simulation method based on the consideration of intact structure along the third dimension (stacking direction) is proposed. We introduce the concept of layer group for a comprehensive understanding from a new perspective. We believe this work will provide unprecedented insight into crystalline structures, which is of great significance to the development of crystallography and material science.

The unique XRD pattern of Rh NSs, which exhibit a three-layer structure with an ABC stacking sequence, was firstly examined. Transmission electron microscopy (TEM) and aberration-corrected scanning transmission electron microscopy (AC-STEM) characterizations reveal that the as-prepared product is dominated by a nanosheet morphology with an average lateral size of around 11 nm (Fig. 2a, Figs. S1a, b, and S2 online). Rh NSs are close-packed crystallographic planes exposed (Fig. S1c, d online), with side view investigations showing an average thickness of 0.56 nm, consisting of 3 atomic layers (Fig. S3 online). The stacking sequence is identi-

\* Corresponding authors.

E-mail addresses: [nanzhang@fjirsm.ac.cn](mailto:nanzhang@fjirsm.ac.cn) (Z.-A. Nan), [haixinlin@xmu.edu.cn](mailto:haixinlin@xmu.edu.cn) (H. Lin), [zxixie@xmu.edu.cn](mailto:zxixie@xmu.edu.cn) (Z. Xie).

<sup>1</sup> These authors contributed equally to this work.

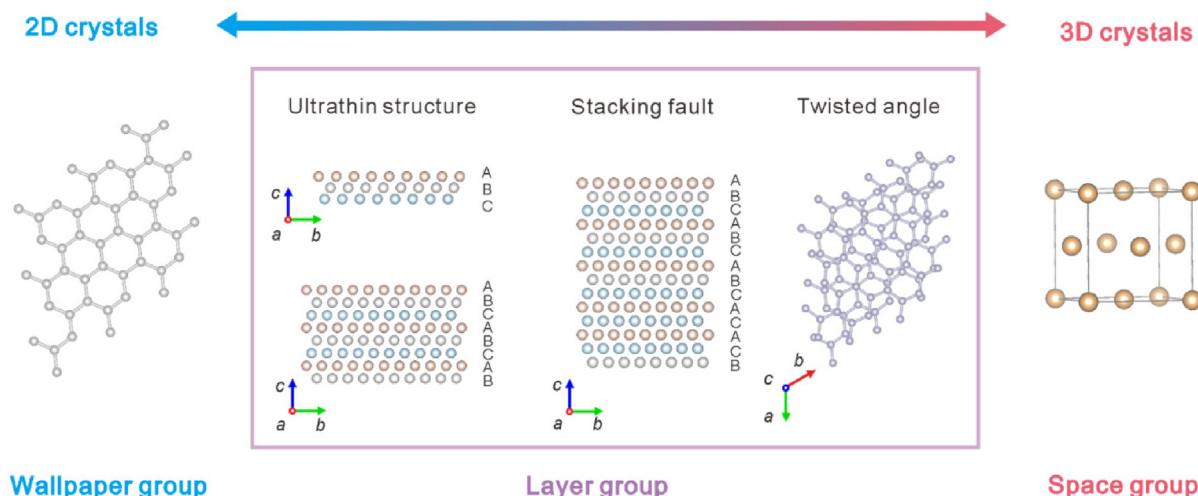


**Fig. 1.** Schematic illustration of crystalline structures with different stacking forms, which are distinct from 2D and 3D crystals.

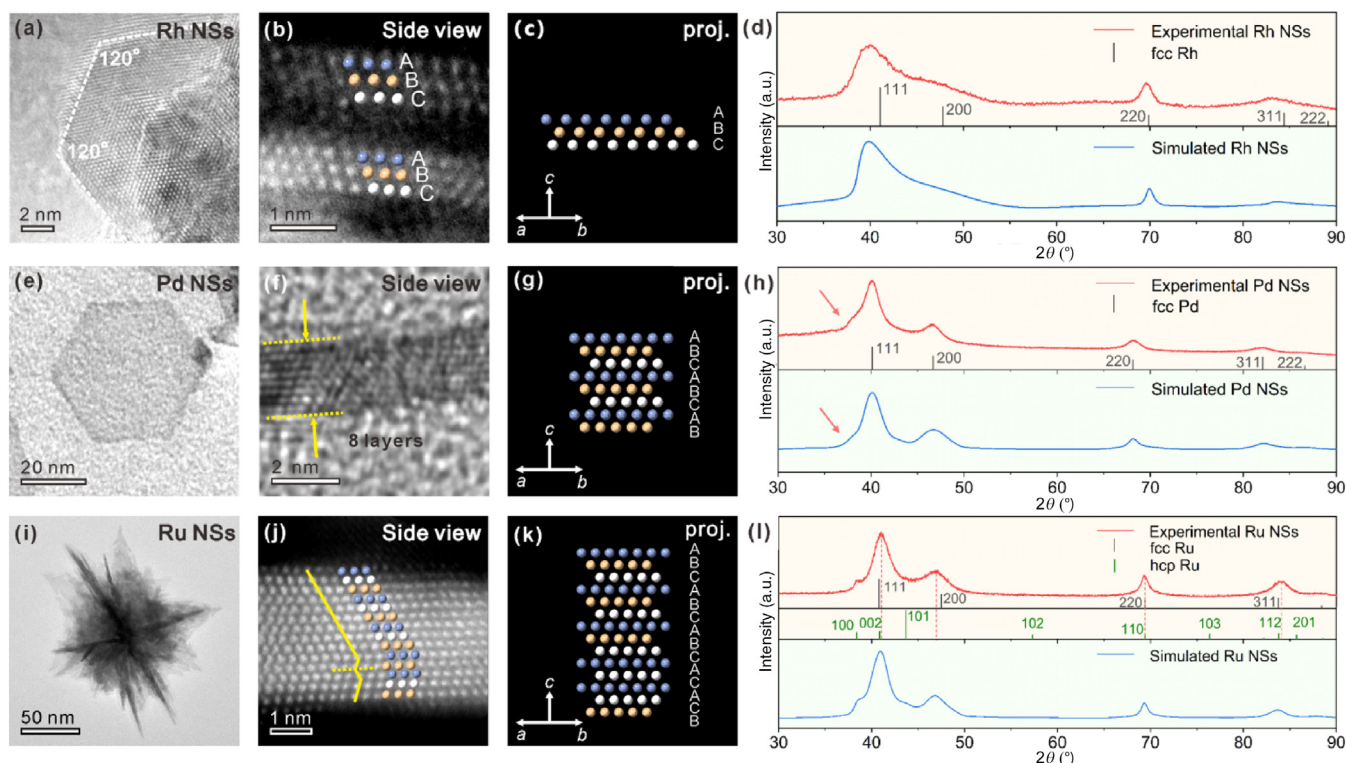


**Fig. 2.** Characterizations of as-prepared metallic NSs. (a, e, i) TEM images of Rh NSs, Pd NSs and Ru NSs, respectively. (b, f, j) AC-STEM and HRTEM images viewed from the side of Rh NSs, Pd NSs, and Ru NSs, respectively. The atomic arrangement sequence is outlined by a yellow solid line and the twinning orientation is marked by a yellow dotted line in Fig. 2j. (c, g, k) Crystal structure models projected from the side of Rh, Pd, and Ru NSs, respectively. (d, h, l) XRD patterns comparisons of experimental results and simulations of Rh, Pd, and Ru NSs, respectively.

defined as ABC, which is the stacking unit of face-centered cubic (fcc) phase (Fig. 2b). The 220 peak of bulk fcc Rh, corresponding to the in-plane diffraction of the close-packed plane, matches the experimental XRD pattern of the ultrathin crystal (Fig. 2d). However, the other diffraction peaks are asymmetric and irregularly offset, with the diffraction intensity around  $40^\circ$  undergoing a rapid increase followed by a slow decline. These diffraction features indicate the symmetry of Rh NSs is distinct from thinned 3D crystals. Therefore, it requires the development of a new analysis method that considers the degrees of freedom in the third dimension. To solve this, we

established a full-structure simulation method (Supplementary Discussion 1 online) for XRD simulation, which is based on a superlattice stacking model intercalating with large vacuum layers (Figs. S4–S6 online). Herein, the one-period with ABC-stacked sequence in the third dimension is considered as the simulation model (Fig. 2c). The simulated diffraction pattern matches well with our experimental data in terms of both peak shape and position (Fig. 2d).

The successful simulation of Rh NSs suggests that ultrathin crystalline materials may possess inherently different XRD fea-

tures compared to the corresponding 3D crystals. To verify this, we conducted XRD simulations with different number of stacked layers referring to 3D fcc and hexagonal closed-packed (hcp) Rh phases, using the close-packing of identical spheres (CPISS) model (Fig. S7 and Supplementary Discussion 2 online). The XRD simulation results exhibit different features compared with 3D fcc (Fig. S7a online). The XRD peak around the  $111_{\text{fcc}}$  peak position adopts an asymmetric shape when the number of layer is smaller than 4, which was also observed in the previous reported 2D materials [8,9]. Furthermore, as the number of layers increases, the appearance of the shoulder peak at around  $38^\circ$  is observed. Based on these simulation results, we speculated that such XRD shoulder peaks would also be observed for materials with more stacking layers. To confirm this, ultrathin Pd NSs consisting of 8 atomic layers were prepared according to the reported methods [10], which exhibit a hexagonal shape with an average thickness of 1.88 nm (Fig. 2e, f and Fig. S8 online). The XRD pattern of Pd NSs exhibits a shoulder peak at about  $38^\circ$ , consistent with our simulated result (Fig. 2h). Following the understanding of the 3-layer Rh NSs, the unique freedom in the third dimension need be considered. By simulating the XRD patterns of Pd NSs with different atomic layer stacking orders (Fig. S9 online), the stacking sequence ABCABCAB was chosen because of the precise matching with the experimental XRD (Fig. 2g, h).

Encouraged by the successful XRD simulations of well-defined ultrathin structures, the examination of ultrathin crystalline materials was extended to 14-layer Ru NSs containing stacking faults in the third dimension. As shown in Fig. 2i (see also Fig. S10 online), TEM characterizations reveal Ru NSs exhibit a range of triangular shapes and assemble into spiky balls. These Ru NSs are about 2.7 nm in thickness, with  $14 \pm 2$  atomic layers (Fig. S11 online). X-ray photoelectron spectroscopy (XPS) analyses show that the Ru element mainly exists in its metallic state (Fig. S12 online). Interestingly, although the XRD pattern of Ru NSs is quite similar to the bulk Ru fcc phase XRD pattern, an abnormal diffraction peak around  $38^\circ$  is observed, which is present in the bulk Ru hcp phase XRD pattern (Fig. 2l and Fig. S13 online). However, the XRD pattern of Ru NSs does not match exactly with either hcp or fcc phases, or a mixtures of them. For instance, the diffraction peaks at about  $41^\circ$  and  $47^\circ$  shift oppositely compared to the  $111_{\text{fcc}}$  and  $200_{\text{fcc}}$  planes of bulk Ru, indicating that these Ru NSs peaks cannot be attributed to the ideal fcc phase. Moreover, although hcp is a stable phase for Ru [11], some typical sets of hcp diffraction peaks, for example  $102_{\text{hcp}}$  and  $103_{\text{hcp}}$  are absent, indicating that Ru NSs cannot be ascribed to the mixed phase of ordered fcc and hcp Ru.

To get deep insight into the XRD patterns, the atomic pair distribution function (PDF) analysis was carried out for the Ru NSs. The PDF analysis indicates the nearest distance between Ru atoms corresponds to metallic Ru with close-packing structure (Figs. S14, S15, and Supplementary Discussion 3 online) [12]. Further AC-STEM investigations show stacking faults typically exist in the fcc close-packing crystal structure along the packing direction (Fig. 2j, k, Figs. S16, S17, and Supplementary Discussion 4 online). For bulk crystals with stacking faults, the powder XRD patterns are usually the same as the corresponding normal crystals, although the translation symmetry is broken due to the stacking faults (Fig. S18 and Supplementary Discussion 5 online). These differences between Ru NSs and bulk 3D structure indicate ultrathin effects are involved. Interestingly, when considering unique freedom in the third dimension of the ultrathin structure, the full structural simulation of XRD patterns matches well with the experimental one (Fig. 2k, l), using intact packing structure in the third dimension according to the AC-STEM observations.

The symmetries of ultrathin crystals can also be varied when the stacking atomic layers are twisted with a specific angle. Examples can be seen by the magic-angle twisted bilayer graphene, in

which the graphene layers are twisted with respect to each other. Herein, four types of bilayer graphenes were constructed and simulated using full-structure method (Fig. S19 online). Compared to the crystal structure without periodicity destruction (AA and AB stacking), the simulated XRD patterns of twisted bilayer graphenes exhibit different XRD features. For example, the peak shapes at around  $43^\circ$  are different, and some secondary diffraction peaks are observed due to the different in-plane periodicities induced by the twisted layers.

From the above three types of ultrathin crystals, we can observe the diffraction differences between ultrathin crystalline materials and traditional 3D crystalline materials, which are proven to be caused by the finite/non-periodic layers along the stacking direction. The symmetry variations induced by the stacking degrees of freedom, are closely related to physical properties, for instance, superconductivity, chirality, and piezoelectricity [13,14]. Therefore, it is essential to accurately describe the symmetries of ultrathin crystalline structures. In mathematics, there is a class of subperiodic groups between 2D and 3D symmetries, named layer groups ( $G_2^3$  groups), which are applied to describe objects in three-dimensional space with translation symmetry in 2D subspace (Table S1 online) [15]. Layer groups can describe well such finite/non-periodic stacking materials in the third dimension on the basic characteristics of 2D lattices. It is therefore appropriate to apply the layer groups for the description of ultrathin crystalline materials. When using layer groups to describe the symmetries of as-prepared nanosheets, the above Rh NSs and Pd NSs can be indexed as layer group  $p\text{-}3m1$ , while Ru NSs can be indexed as layer group  $p3m1$ . For the different stacking patterns of bilayer graphenes, they can be indexed as layer groups  $p6/mmm$ ,  $p\text{-}3m1$ ,  $p622$  and  $p321$ , respectively (Fig. S19 online).

In crystallography, the symmetries of bulk crystals with infinite periodicity are described by 230 space groups, while ideal two-dimensional lattices are described by 17 wallpaper groups. Ultrathin crystalline materials with freedom in the third dimension can be regarded as a form of symmetry breaking due to ultrathin feature in the direction normal to the surface. For example, for bilayer graphene with different twist angles, the point group symmetries are lowered to layer groups  $p622$  or  $p321$  (point group  $D_6$ , or  $D_3$ ) compared to the AA or AB stacking graphite (point groups  $D_{6h}$  or  $D_{3d}$ ) (Fig. S19 online). On the other hand, compared with ideal 2D crystals, ultrathin crystalline materials with freedom in the third dimension possess more symmetry elements in the inter-layer direction, such as inversion centers, mirror plane, 2 and  $2_1$  axes (Supplementary Discussion 6 online). Additionally, the introduction of layer groups for the description of ultrathin crystalline materials, will provide a comprehensive understanding of symmetry-dependent physical properties. For instance, the point group transform from  $D_{6h}$  to  $D_{3h}$  when 3D WSe<sub>2</sub> (space group  $P6_3/mmc$ ) converts to monolayer WSe<sub>2</sub> (layer group  $p\text{-}6m2$ ) (Fig. S20 online), thus the optical second-harmonic generation (SHG) can be detected in non-centrosymmetric monolayer WSe<sub>2</sub> crystals [3]. Therefore, it is necessary to distinguish ultrathin crystalline materials from 2D and 3D crystals, which may help with investigating new symmetry-correlated properties for materials engineering.

In conclusion, from a new point of view, our work shows that ultrathin crystalline materials with freedom in the third dimension, which were generally considered as 2D or thinned 3D materials, are different from 2D and 3D crystals. Three representative types of crystal structures are demonstrated as examples based on crystallographic and mathematical viewpoints. A new full-structure simulation method is established for the analysis of unique diffraction patterns, which are distinct from 2D and 3D crystals, and cannot be well explained before. The successful simulations of XRD patterns further emphasizes the necessity of con-



sidering the degrees of freedom in the third dimension for ultrathin crystalline structures, and layer groups are proposed to be applied to describe this class of structures. Our work is promising for the development of functional materials determined by crystal symmetry and will promote fundamental research in crystallography and material science.

### Conflict of interest

The authors declare that they have no conflict of interest.

### Acknowledgments

This work was supported by the National Key Research and Development Program of China (2020YFB1505802), the National Natural Science Foundation of China (21931009 and 21721001), the Fundamental Research Funds for the Central Universities (20720210016 and 20720210104), and the China Postdoctoral Science Foundation (2020M671939). Additional support was provided by Feringa Nobel Prize Scientist Joint Research Center. We are thankful to Gen Li at Zhongxin Kenong (Shandong) Ecological Agriculture Co., Ltd., in China, Dr. Zier Yan at Rigaku Beijing Corporation in China, and Sixu Peng at Guangxi Normal University in China for the help with data analysis. We are also thankful to Andrés Molina Villarino from Cornell University in USA for revising the English grammar, spelling, and phrasing of the manuscript.

### Author contributions

Hengrui Ma and Qiaorong Jiang conducted the synthesis and characterization of the materials. Hengrui Ma drafted the manuscript and data analysis with the help of Zi-Ang Nan. Gen Li, Yan-yan Jia, and Sheng Dai conducted the AC-STEM characterization. Hengrui Ma and Ruoxin Ning conducted the model construction. Jia-Bao Ji and Zi-Ang Nan conducted the mathematical analysis. Zhenming Cao and Huiqi Li provided important advice during the experimental process. Linzhe Lü provided help with the data analysis. Haixin Lin gave important advice on the data analysis and helped revise the manuscript. Zhaoxiong Xie and Zi-Ang Nan proposed the research project and guided the whole experiment.

### Appendix A. Supplementary materials

Supplementary materials to this short communication can be found online at <https://doi.org/10.1016/j.scib.2023.04.006>.

### References

- [1] Novoselov KS, Geim AK, Morozov SV, et al. Electric field effect in atomically thin carbon films. *Science* 2004;306:666–9.
- [2] Cao Y, Fatemi V, Fang S, et al. Unconventional superconductivity in magic-angle graphene superlattices. *Nature* 2018;556:43–50.
- [3] Lin KQ, Ong CS, Bange S, et al. Narrow-band high-lying excitons with negative-mass electrons in monolayer WSe<sub>2</sub>. *Nat Commun* 2021;12:5500.
- [4] Wu W, Wang L, Li Y, et al. Piezoelectricity of single-atomic-layer MoS<sub>2</sub> for energy conversion and piezotronics. *Nature* 2014;514:470–4.
- [5] Dong Y, Wu Z-S, Ren W, et al. Graphene: a promising 2D material for electrochemical energy storage. *Sci Bull* 2017;62:724–40.
- [6] Gong P, Yu H, Wang Y, et al. Nonlinear optics in the electron-hole continuum in 2D semiconductors: two-photon transition, second harmonic generation and valley current injection. *Sci Bull* 2019;64:1036–43.
- [7] Pi Y, Zhang N, Guo S, et al. Ultrathin laminar Ir superstructure as highly efficient oxygen evolution electrocatalyst in broad pH range. *Nano Lett* 2016;16:4424–30.
- [8] Jiang Y, Cao L, Hu X, et al. Simulating powder X-ray diffraction patterns of two-dimensional materials. *Inorg Chem* 2018;57:15123–32.

- [9] Cao L, Lin Z, Peng F, et al. Self-supporting metal-organic layers as single-site solid catalysts. *Angew Chem Int Ed* 2016;55:4962–6.
- [10] Li Y, Yan Y, Li Y, et al. Size-controlled synthesis of Pd nanosheets for tunable plasmonic properties. *CrystEngComm* 2015;17:1833–8.
- [11] Zhao M, Xia Y. Crystal-phase and surface-structure engineering of ruthenium nanocrystals. *Nat Rev Mater* 2020;5:440–59.
- [12] Billinge Simon JL, Levin I. The problem with determining atomic structure at the nanoscale. *Science* 2007;316:561–5.
- [13] Ago H, Okada S, Miyata Y, et al. Science of 2.5 dimensional materials: paradigm shift of materials science toward future social innovation. *Sci Technol Adv Mater* 2022;23:275–99.
- [14] Zuo Y, Yu W, Liu C, et al. Optical fibres with embedded two-dimensional materials for ultrahigh nonlinearity. *Nat Nanotechnol* 2020;15:987–91.
- [15] Vainsthein BK. Modern crystallography. In: Vainsthein BK, Chernov AA, Vainshtein SLA, editors. *Fundamentals of crystals: symmetry, and methods of structural crystallography*. Berlin: Springer; 1994. p. 53–64.



Hengrui Ma received her B.S. degree from Central China Normal University in 2018. Then she continued to pursuing her Ph.D. degree at Xiamen University under the supervision of Prof. Zhaoxiong Xie. Her research interest is surface structure engineering of noble metal-based nanocrystals and electrocatalysis investigations.



Qiaorong Jiang received his B.S. degree (2014) in Chemistry from Wenzhou University, M.S. degree (2017) and Ph.D. degree (2021) in Chemistry from Xiamen University. He is currently working as a postdoctoral research fellow in Prof. Zhaoxiong Xie's group at Xiamen University. His current research focuses on the controlled synthesis and structure-effect relationship of thermodynamically metastable nanomaterials.



Zi-Ang Nan received his Ph.D. degree from Xiamen University in 2019 under the supervision of Profs. Quan-Ming Wang, Zhaoxiong Xie, and Zhong-Qun Tian. After working as a postdoctoral fellow with Profs. Zhong-Qun Tian, Bing-Wei Mao, and Zhaoxiong Xie at Xiamen University, he joined Xiamen Key Laboratory of Rare Earth Photoelectric Functional Materials in 2023. His current research interest includes crystallography technology, theory and software.



Haixin Lin received his B.S. and Ph.D. degrees from Xiamen University in 2010 and 2016, respectively. He visited Northwestern University from 2013 to 2015, and continued to work as a postdoctoral fellow with Prof. Chad A. Mirkin. He joined Xiamen University as a Professor of Inorganic Chemistry in 2021. His current research interest is the controllable synthesis and assembly of nanomaterials.



Zhaoxiong Xie received his B.S., M.S., and Ph.D. degrees from Department of Chemistry, Xiamen University in 1987, 1990, and 1995, respectively. Since 2002, he holds the position of Professor of Physical Chemistry at Xiamen University. His current research interest focuses on surface/interface chemistry of functional inorganic nanomaterials.